MOLECULAR SUBTYPES AND GENOMIC PROFILE OF PRIMARY CENTRAL NERVOUS SYSTEM LYMPHOMA

Csaba Bödör, PhD[1]; Donát Alpár PhD[1]; Dóra Marosvári, MD[1]; Bence Galik, BS[2]; Hajnalka Rajnai, MD, PhD[1]; Bence Bátai[1]; Ákos Nagy MD[1], Béla Kajtár, MD, PhD[3]; Adrienn Burján, MD[3]; Beáta Deák, MD[4]; Tamás Schneider, MD, PhD[4]; Hussain Alizadeh, MD, PhD[5]; András Matolcsy, MD, PhD[1]; Sebastian Brandner MD, PhD[6]; James Storhoff, PhD[7]; Ning Chen, PhD[7]; MingDong Liu, PhD[7]; Nadeem Ghali, PharmD[8]; Irén Csala, MD, PhD[9]; Attila G. Bagó, MD, PhD[10]; Attila Gyenesei, PhD[2]; Lilla Reiniger MD, PhD[1,11]

1, MTA-SE Momentum Molecular Oncohematology Research Group, 1st Department of Pathology and Experimental Cancer Research, Semmelweis University, Budapest, Hungary; 2, Vienna Biocenter Core Facilities GmbH, Vienna, Austria; 3, Department of Pathology, University of Pécs, Pécs, Hungary; 4, Department of Medical Oncology and Haematology, National Institute of Oncology, Budapest, Hungary; 5, 1st Department of Internal Medicine, Hematology Division, University of Pécs, Pécs, Hungary; 6, Division of Neuropathology, The National Hospital for Neurology and Neurosurgery, University College London Hospitals NHS Foundation Trust and Department of Neurodegenerative Disease, UCL Queen Square Institute of Neurology, London, WC1N 3BG United Kingdom; 7, NanoString Technologies, Seattle, WA, USA; 8, Incyte Corporation, Wilmington, Delaware, USA; 9, Department of Psychiatry and Psychotherapy, Semmelweis University, Budapest, Hungary; 10, Department of Neurooncology, National Institute of Clinical Neurosciences, Budapest, Hungary; 11, SE-NAP Brain Metastasis Research Group, Second Department of Pathology, Semmelweis University, Budapest, Hungary.

Correspondence: Lilla Reiniger: reiniger.lilla@med.semmelweis-univ.hu or Csaba Bödör: bodor.csaba1@med.semmelweis-univ.hu, 1st Department of Pathology and Experimental Cancer Research, Semmelweis University, Üllői út 26, Budapest, Hungary, H-1085.

Tel.: + 36 1 459 1500/4435, FAX: + 36 1 317 1074

Running head title: Molecular subtypes and genomic profile of PCNSL

Conflict of interest: The authors declare no conflict of interest.

Abstract

Primary central nervous system lymphomas (PCNSL) are aggressive non-Hodgkin lymphomas affecting the central nervous system (CNS). Although immunophenotyping studies suggested an uniform activated B-cell (ABC) origin, more recently a spectrum of ABC and germinal center B-cell (GC) cases has been proposed, with the molecular subtypes of PCNSL still being a matter of debate. With the emergence of novel therapies demonstrating different efficacy between the ABC and GC patient groups, precise assignment of molecular subtype is becoming indispensable. To determine the molecular subtype of 77 PCNSL and 17 secondary CNS lymphoma patients, we used the NanoString Lymphoma Subtyping Test (LST), a gene expression-based assay representing a more accurate technique of subtyping compared to standard immunohistochemical (IHC) algorithms. Mutational landscapes of 14 target genes were determined using ultra-deep next-generation sequencing. Using the LST-assay, a significantly lower proportion (80% versus 95%) of PCNSL cases displayed ABC phenotype compared to the IHC-based characterization. The most frequently mutated genes included *MYD88*, *PIM1* and *KMT2D*. In summary, we successfully applied the LST-assay for molecular classification of PCNSL, reporting higher proportion of cases with GC phenotype compared to IHC analyses, leading to a more precise patient stratification potentially applicable in the diagnostic algorithm of PCNSL.

Key words: PCNSL; brain lymphoma; molecular subtype; mutation profiling.

Introduction

Primary central nervous system lymphoma (PCNSL) is a rare malignancy with a particularly aggressive clinical course and poor outcome. Histologically, it is predominantly manifested as diffuse large B-cell lymphoma (DLBCL), which is confined to the central nervous system (CNS) structures (1-3).

It has been almost two decades since the seminal paper by Alizadeh *et al.* changed our perspective by sub-classifying DLBCLs into molecular subgroups including germinal center B-cell (GC) type or activated B-cell (ABC) type, with a small number of "unclassified" (UC) cases (4). This sub-classification has profound prognostic and potential therapeutic implications, with patients in the ABC-type DLBCL group showing significantly inferior outcome (4, 5). The GC/ABC classification of DLBCLs is based on gene expression patterns (GEP) of fresh or fresh-frozen tissues and became the "gold-standard" method for molecular subtype assignment in DLBCL. This discovery was followed by the development of various formalin-fixed paraffin-embedded (FFPE) tissue-based immunohistochemistry (IHC) predictors, including the well-known Hans algorithm, easily applicable in routine diagnostic practice (6-8). However, these IHC-based algorithms showed a poor concordance with each other and the readouts of the gold-standard Affymetrix method (8-10).

The fundamental difference in biology between GC- and ABC-type DLBCL is reflected in different driver oncogenic pathways and mutation targets which also translates in different efficacy of the novel targeted therapies between the two subgroups (11-13). Considering the emerging novel therapies with differential efficacy in the biological subtypes of DLBCL, precise assignment of patients into these subgroups may well become of major clinical importance in the near future. The NanoString Lymphoma Subtyping Test (LST) assay

(NanoString Technologies, Inc., Seattle, USA) was developed to establish an FFPE compatible, gene expression based test for the molecular subtyping of B-cell lymphomas. The LST-assay is based on the expression of 15 target genes and 5 housekeeping genes, and nowadays represents a more accurate technique compared to standard IHC algorithms and demonstrates the best concordance with the gold-standard Affymetrix approach (14).

The molecular subtype of PCNSL has been studied by different methodological approaches with conflicting conclusions. Based on several IHC studies, an ABC-like immunophenotype is typical (15-17), but immunoglobulin heavy chain gene (IGHV) mutational signatures also provide evidence for germinal center exposure, indicating that PCNSL develops from a B-cell that has been exposed to a germinal center influence outside the CNS (18-20). In addition, results of immunophenotyping studies suggest that tumor cells originate from a late germinal center to an early post-germinal center stage (15, 21), while gene expression profiling studies indicate that PCNSLs are distributed among the spectrum of systemic DLBCL with roughly equal proportion of ABC and GC cases (22, 23).

Recent studies profiling the genomic background of PCNSL have identified multiple recurrently mutated genes, including genes harboring putative driver aberrations and others serving as aberrant somatic hypermutation (ASHM) targets (24-30). The most frequently mutated genes include members of the B-cell receptor signaling (i.e. *MYD88*, *CD79B*, *CARD11*), as well as cell cycle/apoptosis regulator (i.e. *TP53*, *CCND3*, *BTG2*, *PIM1*, *CDKN2A*, *ATM*), chromatin (i.e. *KMT2D*) and transcriptional (i.e. *C-MYC*, *PRDM1*, *TBL1XR1*) regulator pathways, with considerable overlap with the mutational targets identified in systemic DLBCL. However, in contrast to nodal DLBCLs, the mutation profiles of PCNSLs of ABC and GC origin do not show considerable differences (29-32).

Since management of PCNSL still represents a significant clinical challenge, both the precise determination of the molecular subtypes and the identification of key genetic alterations are

becoming increasingly important for developing novel therapies and applying a personalized therapeutic approach in the treatment of these patients. In this study, we applied, for the first time, the NanoString LST-assay to determine molecular subgroups of a large cohort of PCNSL patients and performed complementary targeted mutation profiling on a subset of these cases.

Materials and Methods

FFPE brain biopsy specimens of 81 patients with PCNSL and 18 patients with secondary central nervous system lymphoma (SCNSL) were analyzed in this study. Tissue samples were obtained from three centers: (i) 1st Department of Pathology and Experimental Cancer Research, Semmelweis University, Budapest, Hungary; (ii) Department of Pathology, University of Pécs, Pécs, Hungary and (iii) Division of Neuropathology, The National Hospital for Neurology and Neurosurgery, University College London Hospitals, United Kingdom, through the UK Brain Archive Information Network (BRAIN UK). Permissions to use the archived tissue have been obtained from the Local Ethical Committee (TUKEB-1552012) and from BRAIN UK (Ref.: 16/018), and the study was conducted in accordance with the Declaration of Helsinki. Clinical data of the patients and information on the molecular subtype as determined by IHC during the routine diagnostic workup are summarized in Supplementary Table 1. Survival data was available in 65 PCNSL and 17 SCNSL cases, with treatment data available in 46 PCNSL and 12 SCNSL cases, respectively (Supplementary Table 1.).

Molecular subtyping using the NanoString LST-assay

RNA isolation from 77 PCNSL and 17 SCNSL samples was performed using the RecoverAll™ kit (Life Technologies/Ambion, Inc, Foster City USA) according to the manufacturer's instructions. Molecular subtype was determined using the Research Use Only version of the LST-assay on the nCounter® Analysis System (NanoString Technologies, Inc., Seattle, USA).

The LST-assay measures 15 signature genes and 5 housekeeping genes in RNA samples isolated from FFPE DLBCL tumor tissue, as described previously (14). For each RNA sample, a Linear Predictor Score (LPS) is calculated using a weighted sum of the gene expression. The LPS is compared against thresholds that define LPS value ranges for the assignment of ABC or GC subtype, or Unclassified within an equivocal zone.

Ultra-deep next-generation sequencing of 14 target genes

Genomic DNA was extracted from 64 PCNSL and 12 SCNSL samples using the FFPE Tissue Kit (Qiagen, N.V., Venlo, Netherlands) following the manufacturer's instructions. DNA samples isolated from five non-malignant tissue specimens were used as negative controls. Mutation profiles of 14 genes including *CARD11, CCND3, CD79B, CSMD2, CSMD3, IRF4, KMT2D, C-MYC, MYD88, PAX5, PIM1, PRDM1, PTPRD* and *TP53* were determined by targeted ultra-deep next-generation sequencing (NGS) using the TruSeq Custom Amplicon dual-strand approach (Illumina, Inc., San Diego, USA). This protocol is specifically designed for FFPE samples and uses two mirrored sets of locus-specific oligos generating matching complementary, strand-specific amplicon libraries. Completely independent preparation of the two sample-specific libraries (A and B) and sequencing with unique barcodes allow for a subsequent bioinformatics correction of errors/bias conferred by FFPE fixation. After quality control and equimolar pooling, libraries were sequenced on a HiSeq 4000 Instrument using 150bp paired-end chemistry.

Bioinformatics workflow

During data preprocessing, sequencing reads were mapped to the *Homo sapiens* GRCh37 genome build using BWA v0.7.13 aligner from the BaseSpace Sequence Hub (Illumina, Inc., San Diego, USA). BAM files were sorted and indexed by SAMtools v1.7 module

(http://samtools.sourceforge.net) and GATK v4.0 tool Base Quality Score Recalibration (Broad Institute, Cambridge, USA) was run on each individual library to detect and correct systematic sequencing errors. SNP and INDEL calling was performed with LoFreq v2.1 variant-caller (33) that considers all dataset features, also including base-call qualities, mapping problems or base/INDEL misalignments, which are commonly ignored by other methods or only used for filtering. Assignment of each detected variant with a p-value allowed for a rigorous control of false positive findings. Raw variants, detected by LoFreq v2.1, were functionally annotated using SnpEff v4.3i as well as ANNOVAR v2017Jul17 tools, with the latter one also including up-to-date information from COSMIC, avSNP and CLINVAR databases (34, 35). After the final annotation step, somatic variants detected in sample-specific, matching individual libraries (A and B) were combined based on genomic position and allele type using an in-house R script (version 3.4.3 (2017-11-30)), and variants exclusively identified in both libraries A and B were considered as true aberrations. A subset of somatic variants with variant allele frequency of >20% was validated by bidirectional Sanger sequencing.

Statistical analysis

Kaplan-Meier survival curves and log-rank tests were performed to compare survival times between groups using GraphPad PRISM v. 5.0 software (GraphPad Software, San Diego, USA). Pearson Chi-square test or Fisher's exact test were used to analyze categorical data. P values 0.05 or below were considered statistically significant.

Results

Molecular subtypes

Using the Hans algorithm, 95% of the PCNSL cases (73/77) showed ABC (non-GC) phenotype, with 5% of the patients (4/77) presenting with GC phenotype. In contrast, the LST-assay identified only 80.5% (62/77) of the cases as ABC subtype, with 13% (10/77) GC and 6.5% (5/77) UC subtypes, respectively. As for the SCNSL cases, 47% (8/17) showed ABC and 53% (9/17) showed GC phenotype with the Hans algorithm. The ratio was identical using the LST-assay, with 47% (8/17) ABC and 53% (9/17) GC subtypes.

The sub-classification obtained with the LST-assay showed discordant readouts in 16% (15/94) of all analyzed cases (13/77 of PCNSL and 2/17 of SCNSL cases) as compared to the IHC results. 12.5% (12/94) of the cases classified as ABC by the Hans algorithm showed a different readout when analyzed using the LST-assay, with 7 cases assigned to the GC group and 5 unclassified cases; while only one (1%) IHC-GC case was classified as ABC using the LST-assay (Figure 1). In the SCNSL group, only a single GC and a single ABC case did not match when comparing the readouts of the Hans algorithm and the LST-assay. Taken together, using the LST-assay, a significantly lower proportion of cases (80.5% versus 95%, p=0.0219) displayed an ABC phenotype in PCNSL.

The survival of the patients with PCNSL and SCNSL did not show a significant difference (p=0.1970) (Figure 2A). Interestingly, the molecular subtypes did not have an impact on the survival of patients, with overall survival showing no differences between the GC and ABC subtype neither in the entire cohort (p=0.3981) nor in the PCNSL cases (p=0.8727) (Figures 2B and 2C).

Mutation profiles

A total of 239 mutations were detected across the 76 brain lymphomas with variant allele frequencies (VAF) ranging between 1.8 and 96.2% with a mean value of 41.4% (Supplementary table 2). The vast majority (81%, 194/239) of the mutations presented with a VAF higher than 20% (Supplementary Figure 1).

We detected a total of 210 somatic mutations in the 64 PCNSL cases across the 14 genes analyzed, with an average of 3.3 mutations per case ranging between 0 and 10 (Supplementary table 2). The distribution of the mutations was as follows: missense mutations: 75.2% (158/210), mutations affecting 5 or 3 prime UTR regions: 11.4% (24/210), mutations at splice sites: 7.6% (16/210), in frame deletions: 3.3% (7/210), frameshift mutations: 1.9% (4/210) and nonsense mutations: 0.5% (1/210). Individual cases harbored mutations in 2.6 genes on average, ranging between 0 and 5.

The most frequently mutated genes in the PCNSL cohort included *MYD88* (66%), *PIM1* (41%), *KMT2D* (31%) and *PRDM1* (30%). The mutation frequencies in the remaining genes were as follows: *C-MYC* (19%), *IRF4* (19%), *CD79B* (17%), *TP53* (11%), *CCND3* (9%), *CARD11* (8%), *PAX5* (3%), *CSMD2* (3%) and *CSMD3* (3%). No mutation was found in *PTPRD* gene (Figures 3 and 4A).

In the 12 SCNSL cases, a total of 29 somatic mutations were detected, with an average of 2.4 mutations per case ranging between 0 and 5 (Supplementary table 2). The distribution of the mutations was as follows: missense mutations: 72.4% (21/29), mutations affecting 5 or 3 prime UTR regions: 20.7% (6/29), frameshift mutations: 3.5% (1/29) and mutations at splice sites: 3.5% (1/29). Individual cases harbored mutations in 1.8 genes on average, ranging between 0 and 4.

PRDM1 (50%), followed by *MYD88* (42%) and *PIM1* (25%) were the most frequently mutated target genes in the SCNSL cohort. The mutations frequencies in the remaining genes proved to be lower: *KMT2D* (17%), *CD79B* (8%), *IRF4* (8%), *CCND3* (8%), *C-MYC* (8%), *TP53* (8%) and *PAX5* (8%). No mutation was identified in *CARD11*, *CSMD2, CSMD3* and *PTPRD* genes (Figures 3 and 4A).

Correlation of mutation profiles and molecular subtypes

Considering all brain lymphomas, we observed an enrichment of *MYD88* (67% vs 46%), *PIM1* (39% vs 23%), *IRF4* (20% vs 8%) and *MYC* (19% vs 8%) mutations in cases with ABC subtype, with *CD79B*, *CARD11*, *CSMD2* and *CSMD3* mutations being present exclusively in ABC cases (19%, 9%, 4% and 4% vs 0% for the four genes, respectively). On the other hand, mutations of *TP53* (15% vs 6%) and *PAX5* (15% vs 2%) appeared more frequent in GC cases. *PRDM1*, *KMT2D* and *CCND3* genes showed similar mutational frequencies by comparing the GC and ABC cases (Figures 3 and 4B).

In PCNSL, enrichment of *PIM1* mutations was observed (41% vs 20%) in cases with ABC subtype, with *IRF4*, *CD79B*, *MYC*, *CARD11*, *CSMD2* and *CSMD3* mutations being present exclusively in ABC cases (22%, 20%, 20%, 10%, 4% and 4% vs 0% for the six genes, respectively). In PCNSL cases with GC subtype, mutations of *TP53* (20% vs 6%), *PAX5* (20% vs 2%) and *CCND3* (20% vs 8%) appeared more frequent compared to the ABC cases. *MYD88*, *PRDM1* and *KMT2D* genes showed similar mutational frequencies across the two subtypes (Figures 3 and 4C).

Despite the apparent enrichment of mutations, none of these differences reached statistical significance when compared between the GC and ABC groups (data not shown).

Discussion

Clinical management of PCNSL patients is still challenging (36), with considerably worse outcomes compared to nodal DLBCLs, highlighting an unmet need for novel biomarkers and therapies. Precise assignment of individual cases into the biologically distinct ABC or GC molecular subtype categories originally described by Alizadeh *et al.* (4), complemented with mutation analysis of actionable target genes may pave the road towards a more effective patient stratification method and personalized application of targeted therapies (11, 12).

Historically, the IHC based studies suggested an ABC cell of origin in the vast majority of PCNSL cases (15-17); however IHC reportedly shows poor concordance with the COO readouts of the gold-standard GEP method (8, 9). In contrast, a gene expression profiling study suggested a rather continuous distribution of PCNSLs among the ABC-, GC- and non-ABC/non-GC-subgroups (23). Recently, the NanoString LST-assay emerged as the most reliable and highly reproducible approach to determine the molecular subtype from FFPE tissues, as successfully demonstrated on a large cohort of nodal DLBCLs (14). Although not yet adopted for routine application, the LST-assay is being used in clinical trials for patient stratification and clinical decision making in DLBCL (37, 38).

In this study, we successfully applied for the first time the NanoString LST-assay for molecular subtyping using FFPE derived RNA samples from a large cohort of patients with brain lymphoma including 77 PCNSL and 17 SCNSL cases. Interestingly, this molecular subtyping revealed a higher proportion of cases with a GC subtype compared to the parallel IHC analysis (13% vs 5%), representing a considerably higher proportion as previously appreciated in the literature (15-21). We believe that these results may better reflect the genuine biology of the cases, as the NanoString LST-assay seems to represent the most reliable approach to determine molecular subgroups, compared to the original gold standard GEP method (14). Unexpectedly, in our study the molecular subtypes did not have a clinically significant impact on the survival

of patients. This may potentially be caused by the heterogeneous nature of the treatment regimens applied for our patient cohort.

The genomic profile of PCNSL has only been dissected recently, using various next-generation sequencing technologies. These studies of smaller patient cohorts revealed a similar mutational burden and profile to that of the nodal DLBCLs, with predominant mutations of the BCR/NFκB pathway (24-30). Here, we performed a complementary targeted genomic profiling of 14 genes in 64 PCNSL and 12 SCNSL patients, focusing on actionable mutation targets and genes with potential prognostic impact. In both primary and secondary brain lymphoma cohorts the most frequently mutated genes included *MYD88*, *PIM1*, *KMT2D* and *PRDM1,* followed by *IRF4, MYC* and *CD79B*. Mutation frequencies of the individual genes observed in this study are in line with previously published data; however' those studies have reported a wide range of mutational frequencies across these genes analyzed (24-30, 39-41). This can most likely be explained by the heterogeneity in the type and depth of the sequencing approaches (whole genome/exome sequencing versus targeted resequencing of selected genes), type of the analyzed material (fresh frozen versus FFPE) and the difference between the bioinformatics pipelines and variant calling methods. Here, in addition to a strict variant calling algorithm, we utilized the so called dual-strand approach, which in actuality represents two independent sequencing experiments, allowing for proper error correction, a critical step when dealing with NGS data obtained from FFPE material.

The most frequently mutated gene in our study, *MYD88* (66%) was found to be frequently mutated in other PCNSL studies as well (24-30, 39, 41); however' only a modest *MYD88* mutation frequency of 10-20% was reported in nodal DLBCLs with *MYD88* mutations restricted to the non-GCB subtype (42). Interestingly, in our PCNSL cohort, *MYD88* also emerged in the GC subtype with similar distribution across the GC and ABC subtypes. This may be of potential therapeutic relevance, as the Bruton's tyrosine kinase inhibitor ibrutinib

demonstrated clinical efficacy in 37% of nodal ABC-DLBCLs, especially in cases with concurrent *MYD88* and *CD79B* mutations (43). In our cohort, ten patients were identified with simultaneous *MYD88* and *CD79B* mutations. Nevertheless, Grommes *et al.*, in a phase I trial reported clinical responses in 10 of 13 patients with relapsed PCNSL with *MYD88* mutations representing the most important genomic determinants of ibrutinib response (44). Interestingly, all patients achieving a complete remission carried only *MYD88* mutations while cases with concurrent *MYD88* and *CD79B* mutations achieved only partial remission only. As expected, *CARD11* mutations were associated with ibrutinib resistance. In our cohort, *CARD11* mutations were detected in 10% of the PCNSL patients. Based on these preliminary data and mutation frequencies observed in our study, ibrutinib may be a promising therapeutic modality for almost half (46%, 35/76) of the patients (cases with *MYD88* and without *CARD11* or *CD79B* mutations), irrespective of the subtype of the cases.

Of note, mutations in genes involved in CNS development were exclusively detected in PCNSL patients. Three percent of the cases harbored mutations in *CSMD2* and *CSMD3* genes, but no mutation was found in the *PTPRD* gene. Although less frequent in our cohort than previously described (25), these mutations may contribute to the emergence of lymphoma primarily in the CNS.

Comparing the mutation frequencies between the GC and ABC subtypes defined by the LST-assay, the mutation patterns observed in PCNSL (as well as SCNSL) do not follow the ones documented in nodal DLBCLs (31, 45-47). While mutations of *CD79B*, *CARD11*, *CSMD2* and *CSMD3* were exclusively detected in ABC cases, differences in mutation frequencies of e.g. *MYD88*, *PIM1* and *KMT2D* between the GC and ABC did not reach statistical significance. This may support the hypothesis that PCNSL represents a distinct clinical entity irrespective of the cell of origin classification as proposed by Fukumura *et al.* (29).

Considering our increasing knowledge on the genomic complexity of PCNSL and emergence of novel therapies with differential activity in the GC and ABC patient groups, precise assignment of molecular subtypes using routinely available FFPE tissues and complementary mutation analysis of the actionable mutation targets will most likely support and drive personalized therapeutic decisions during the management of PCNSL patients. Certainly, the costs associated with these molecular assays would represent a significant financial burden in the clinical setting at the moment; therefore, may still be some time away from clinical implementation, with large scale prospective clinical trials required to confirm the utility of these approaches in the routine diagnostic workflows.

References

1.   Hochberg FH, Miller DC. Primary central nervous system lymphoma. Journal of neurosurgery 1988;686:835-53

2.   O'Neill BP, Illig JJ. Primary central nervous system lymphoma. Mayo Clinic proceedings 1989;648:1005-20

3.   Kluin PM DM, Ferry JA. Primary diffuse large B-cell lymphoma of the CNS. In: Swerdlow SH, Campo E, Harris NL, et al., eds. WHO classification of tumours of haematopoietic and lymphoid tissues, Revised 4th Edition. Lyon: International Agency for Research on Cancer 2017: 300-2

4.   Alizadeh AA, Eisen MB, Davis RE, et al. Distinct types of diffuse large B-cell lymphoma identified by gene expression profiling. Nature 2000;4036769:503-11

5.   Wright G, Tan B, Rosenwald A, et al. A gene expression-based method to diagnose clinically distinct subgroups of diffuse large B cell lymphoma. Proc Natl Acad Sci U S A 2003;10017:9991-6

6.   Hans CP, Weisenburger DD, Greiner TC, et al. Confirmation of the molecular classification of diffuse large B-cell lymphoma by immunohistochemistry using a tissue microarray. Blood 2004;1031:275-82

7.   Choi WW, Weisenburger DD, Greiner TC, et al. A new immunostain algorithm classifies diffuse large B-cell lymphoma into molecular subtypes with high accuracy. Clin Cancer Res 2009;1517:5494-502

8.   Meyer PN, Fu K, Greiner TC, et al. Immunohistochemical methods for predicting cell of origin and survival in patients with diffuse large B-cell lymphoma treated with rituximab. J Clin Oncol 2011;292:200-7

9.   Gutierrez-Garcia G, Cardesa-Salzmann T, Climent F, et al. Gene-expression profiling and not immunophenotypic algorithms predicts prognosis in patients with diffuse large B-cell lymphoma treated with immunochemotherapy. Blood 2011;11718:4836-43

10.   Coutinho R, Clear AJ, Owen A, et al. Poor concordance among nine immunohistochemistry classifiers of cell-of-origin for diffuse large B-cell lymphoma: implications for therapeutic strategies. Clin Cancer Res 2013;1924:6686-95

11.   Karmali R, Gordon LI. Molecular Subtyping in Diffuse Large B Cell Lymphoma: Closer to an Approach of Precision Therapy. Curr Treat Options Oncol 2017;182:11

12.   Sujobert P, Salles G, Bachy E. Molecular Classification of Diffuse Large B-cell Lymphoma: What Is Clinically Relevant? Hematol Oncol Clin North Am 2016;306:1163-77

13.   Nowakowski GS, Feldman T, Rimsza LM, et al. Integrating precision medicine through evaluation of cell of origin in treatment planning for diffuse large B-cell lymphoma. Blood Cancer J 2019;96:48

14.   Scott DW, Wright GW, Williams PM, et al. Determining cell-of-origin subtypes of diffuse large B-cell lymphoma using gene expression in formalin-fixed paraffin-embedded tissue. Blood 2014;1238:1214-7

15.   Camilleri-Broet S, Criniere E, Broet P, et al. A uniform activated B-cell-like immunophenotype might explain the poor prognosis of primary central nervous system lymphomas: analysis of 83 cases. Blood 2006;1071:190-6

16.   Liu J, Wang Y, Liu Y, et al. Immunohistochemical profile and prognostic significance in primary central nervous system lymphoma: Analysis of 89 cases. Oncol Lett 2017;145:5505-12

17.   Raoux D, Duband S, Forest F, et al. Primary central nervous system lymphoma: immunohistochemical profile and prognostic significance. Neuropathology 2010;303:232-40

18.   Thompsett AR, Ellison DW, Stevenson FK, et al. V(H) gene sequences from primary central nervous system lymphomas indicate derivation from highly mutated germinal center B cells with ongoing mutational activity. Blood 1999;945:1738-46

19.   Montesinos-Rongen M, Kuppers R, Schluter D, et al. Primary central nervous system lymphomas are derived from germinal-center B cells and show a preferential usage of the V4-34 gene segment. Am J Pathol 1999;1556:2077-86

20.   Larocca LM, Capello D, Rinelli A, et al. The molecular and phenotypic profile of primary central nervous system lymphoma identifies distinct categories of the disease and is consistent with histogenetic derivation from germinal center-related B cells. Blood 1998;923:1011-9

21.   Sugita Y, Tokunaga O, Nakashima A, et al. SHP-1 expression in primary central nervous system B-cell lymphomas in immunocompetent patients reflects maturation stage of normal B cell counterparts. Pathol Int 2004;549:659-66

22.   Rubenstein JL, Fridlyand J, Shen A, et al. Gene expression and angiotropism in primary CNS lymphoma. Blood 2006;1079:3716-23

23.   Montesinos-Rongen M, Brunn A, Bentink S, et al. Gene expression profiling suggests primary central nervous system lymphomas to be derived from a late germinal center B cell. Leukemia 2008;222:400-5

24.   Bruno A, Boisselier B, Labreche K, et al. Mutational analysis of primary central nervous system lymphoma. Oncotarget 2014;513:5065-75

25.   Vater I, Montesinos-Rongen M, Schlesner M, et al. The mutational pattern of primary lymphoma of the central nervous system determined by whole-exome sequencing. Leukemia 2015;293:677-85

26.   Braggio E, Van Wier S, Ojha J, et al. Genome-Wide Analysis Uncovers Novel Recurrent Alterations in Primary Central Nervous System Lymphomas. Clin Cancer Res 2015;2117:3986-94

27.   Nakamura T, Tateishi K, Niwa T, et al. Recurrent mutations of CD79B and MYD88 are the hallmark of primary central nervous system lymphomas. Neuropathol Appl Neurobiol 2016;423:279-90

28.   Chapuy B, Roemer MG, Stewart C, et al. Targetable genetic features of primary testicular and primary central nervous system lymphomas. Blood 2016;1277:869-81

29.   Fukumura K, Kawazu M, Kojima S, et al. Genomic characterization of primary central nervous system lymphoma. Acta Neuropathol 2016;1316:865-75

30.   Zhou Y, Liu W, Xu Z, et al. Analysis of Genomic Alteration in Primary Central Nervous System Lymphoma and the Expression of Some Related Genes. Neoplasia 2018;2010:1059-69

31.   Kraan W, Horlings HM, van Keimpema M, et al. High prevalence of oncogenic MYD88 and CD79B mutations in diffuse large B-cell lymphomas presenting at immune-privileged sites. Blood Cancer J 2013;3:e139

32.   Yamada S, Ishida Y, Matsuno A, et al. Primary diffuse large B-cell lymphomas of central nervous system exhibit remarkably high prevalence of oncogenic MYD88 and CD79B mutations. Leuk Lymphoma 2015;567:2141-5

33.   Wilm A, Aw PP, Bertrand D, et al. LoFreq: a sequence-quality aware, ultra-sensitive variant caller for uncovering cell-population heterogeneity from high-throughput sequencing datasets. Nucleic Acids Res 2012;4022:11189-201

34.   Cingolani P, Platts A, Wang le L, et al. A program for annotating and predicting the effects of single nucleotide polymorphisms, SnpEff: SNPs in the genome of Drosophila melanogaster strain w1118; iso-2; iso-3. Fly (Austin) 2012;62:80-92

35.   Wang K, Li M, Hakonarson H. ANNOVAR: functional annotation of genetic variants from high-throughput sequencing data. Nucleic Acids Res 2010;3816:e164

36.   Grommes C, Rubenstein JL, DeAngelis LM, et al. Comprehensive Approach to Diagnosis and Treatment of Newly Diagnosed Primary CNS Lymphoma. Neuro Oncol 2018

37.   Nowakowski GS, Chiappella A, Witzig TE, et al. ROBUST: Lenalidomide-R-CHOP versus placebo-R-CHOP in previously untreated ABC-type diffuse large B-cell lymphoma. Future Oncol 2016;1213:1553-63

38.   Araf S, Korfi K, Rahim T, et al. Advances in the molecular diagnosis of diffuse large B-cell lymphoma in the era of precision medicine. Expert Rev Mol Diagn 2016;1610:1093-102

39.   Gonzalez-Aguilar A, Idbaih A, Boisselier B, et al. Recurrent mutations of MYD88 and TBL1XR1 in primary central nervous system lymphomas. Clin Cancer Res 2012;1819:5203-11

40.   Courts C, Montesinos-Rongen M, Brunn A, et al. Recurrent inactivation of the PRDM1 gene in primary central nervous system lymphoma. J Neuropathol Exp Neurol 2008;677:720-7

41.   Zheng M, Perry AM, Bierman P, et al. Frequency of MYD88 and CD79B mutations, and MGMT methylation in primary central nervous system diffuse large B-cell lymphoma. Neuropathology 2017;376:509-16

42.   Ngo VN, Young RM, Schmitz R, et al. Oncogenically active MYD88 mutations in human lymphoma. Nature 2011;4707332:115-9

43.   Wilson WH, Young RM, Schmitz R, et al. Targeting B cell receptor signaling with ibrutinib in diffuse large B cell lymphoma. Nat Med 2015;218:922-6

44.   Grommes C, Pastore A, Palaskas N, et al. Ibrutinib Unmasks Critical Role of Bruton Tyrosine Kinase in Primary CNS Lymphoma. Cancer Discov 2017;79:1018-29

45.   Dubois S, Viailly PJ, Bohers E, et al. Biological and Clinical Relevance of Associated Genomic Alterations in MYD88 L265P and non-L265P-Mutated Diffuse Large B-Cell Lymphoma: Analysis of 361 Cases. Clin Cancer Res 2017;239:2232-44

46.   Davis RE, Ngo VN, Lenz G, et al. Chronic active B-cell-receptor signalling in diffuse large B-cell lymphoma. Nature 2010;4637277:88-92

47.   Kuo HP, Ezell SA, Hsieh S, et al. The role of PIM1 in the ibrutinib-resistant ABC subtype of diffuse large B-cell lymphoma. Am J Cancer Res 2016;611:2489-501

FIGURE LEGENDS

FIGURE 1. The NanoString LST readouts are illustrated in form of a gene expression heat map with the 15 target genes contributing to the model. *Abbreviations: ABC: activated B-cell; GC: germinal center; IHC: immunohistochemistry; PCNSL: primary central nervous system lymphoma; SCNSL: secondary central nervous system lymphoma; UC: unclassified.*

FIGURE 2. Effect of **(A)** the primary or secondary nature and **(B-C)** molecular subtypes on the survival of patients with primary and secondary central nervous system lymphomas. No survival difference was observed between PCNSL and SCNSL or cases with ABC or GC categories. UC cases are not presented on the graphs B and C. *Abbreviations: ABC: activated B-cell; GC: germinal center; mut: mutant; n: number; PCNSL: primary central nervous system lymphoma; SCNSL: secondary central nervous system lymphoma; UC: unclassified.*

FIGURE 3. Illustrated are the mutation patterns of the 14 genes identified in 76 primary and secondary central nervous system lymphomas by next-generation sequencing, and molecular subtypes of 71 and 73 cases as defined by the NanoString LST-assay and the Hans algorithm using immunohistochemistry, respectively. *Abbreviations: ABC: activated B-cell; ASHM: aberrant somatic hypermutation; BCR: B-cell receptor; GC: germinal center; IHC: immunohistochemistry; na: not available; PCNSL: primary central nervous system lymphoma; SCNSL: secondary central nervous system lymphoma; UC: unclassified.*

FIGURE 4. Comparison of mutation profiles between **(A)** primary and secondary central nervous system lymphomas, **(B)** all brain lymphomas of activated B-cell type (ABC) versus germinal center B-cell type (GC) and **(C)** primary brain lymphomas of ABC versus GC type. *Abbreviations: ABC: activated B-cell; GC: germinal center; NANO: NanoString; PCNSL: primary central nervous system lymphoma; SCNSL: secondary central nervous system lymphoma.*
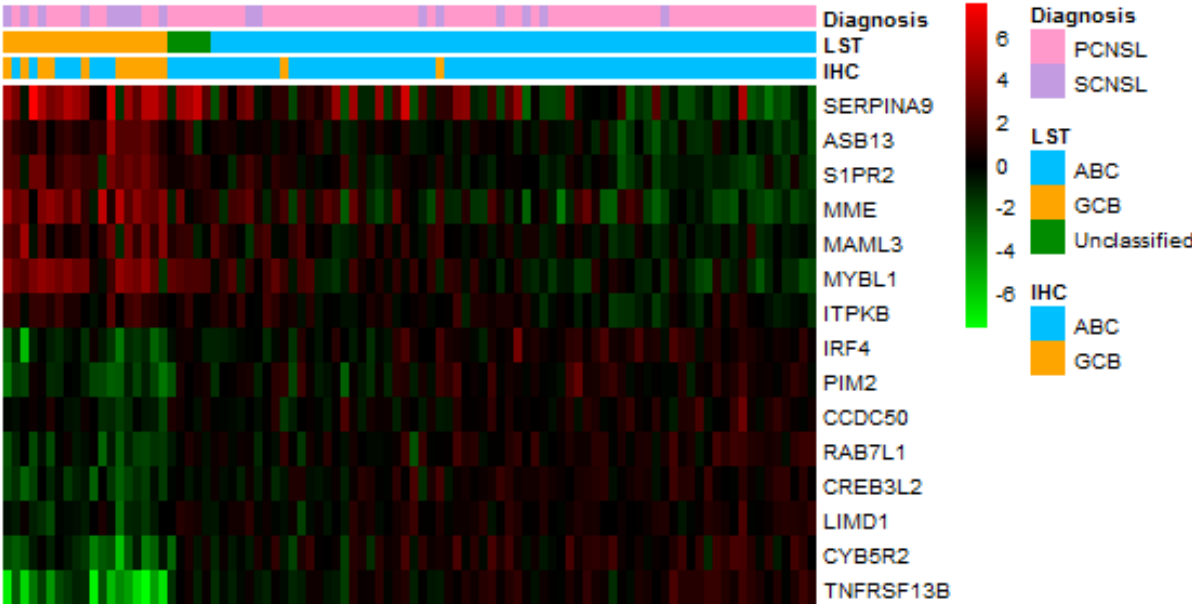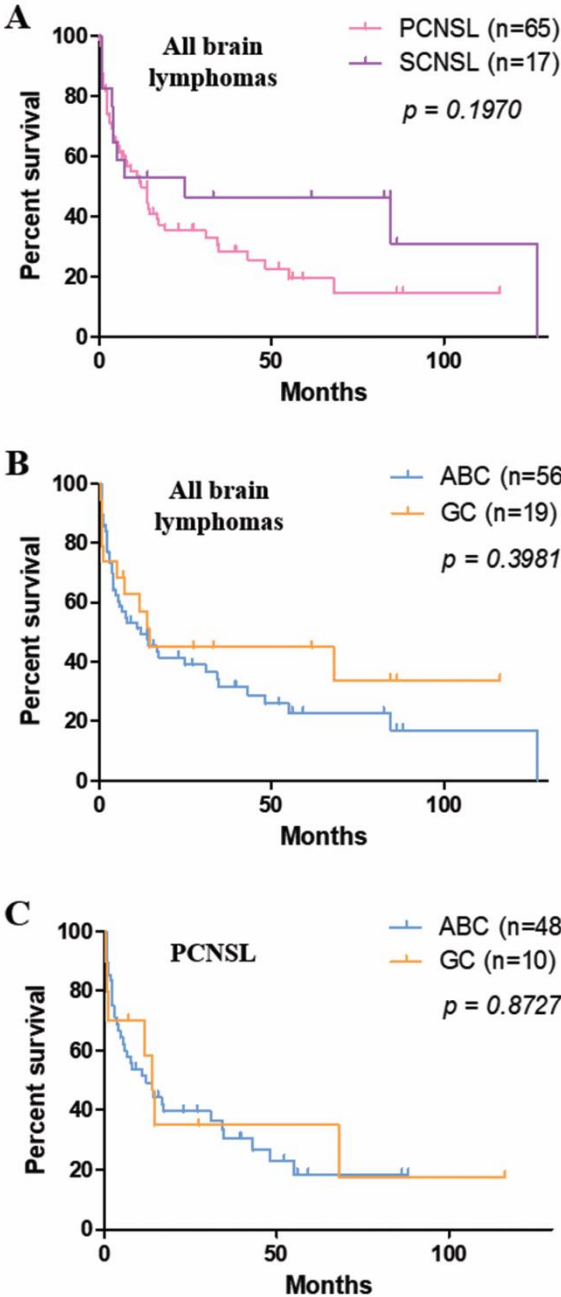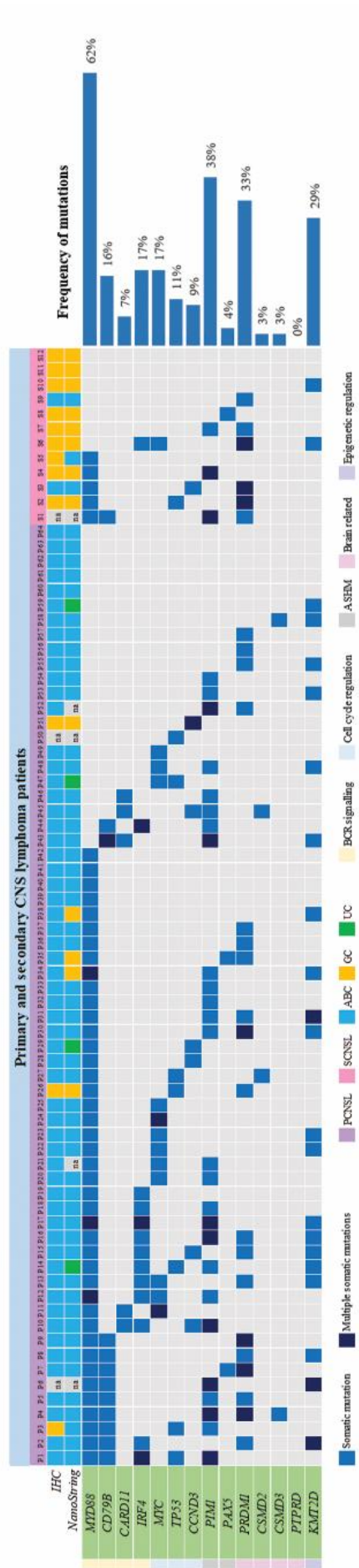
FIGURE 1.

FIGURE 2.

FIGURE 3.

FIGURE 4.

A
PCNSL versus SCNSL

66%	MYD88	42%
41%	PIM1	25%
31%	KMT2D	17%
30%	PRDM1	50%
19%	IRF4	8%
19%	MYC	8%
17%	CD79B	8%
11%	TP53	8%
9%	CCND3	8%
8%	CARD11	0%
3%	PAX5	8%
3%	CSMD2	0%
3%	CSMD3	0%
0%	PTPRD	0%

■ PCNSL   ■ SCNSL

B
All brain lymphomas

67%	MYD88	46%
39%	PIM1	23%
33%	PRDM1	38%
28%	KMT2D	31%
20%	IRF4	8%
19%	CD79B	0%
19%	MYC	8%
9%	CARD11	0%
9%	CCND3	8%
6%	TP53	15%
4%	CSMD2	0%
4%	CSMD3	0%
2%	PAX5	15%
0%	PTPRD	0%

■ ABC   ■ GC

C
PCNSL

67%	MYD88	80%
41%	PIM1	20%
31%	PRDM1	40%
29%	KMT2D	40%
22%	IRF4	0%
20%	CD79B	0%
20%	MYC	0%
10%	CARD11	0%
8%	CCND3	20%
6%	TP53	20%
4%	CSMD2	0%
4%	CSMD3	0%
2%	PAX5	20%
0%	PTPRD	0%

■ ABC   ■ GC